J. Min. Metall. Sect. B-Metall. 55 (1) B (2019) 55 - 63

Journal of Mining and Metallurgy,
Section B: Metallurgy

HIGH TEMPERATURE CORROSION OF COMMERCIAL FeCrAl ALLOYS (KANTHAL AF) IN NITROGEN GAS

S. Veskovič – Bukudur [a], J. Kovač [b], B. Karpe [c*], P. Umek [b], A. Nagode [c], R. Cerc – Korošec [d], M. Bizjak [c]

[a] Hidria d.o.o., Idrija, Slovenia
[b] Institute Josef Stefan, Ljubljana, Slovenia
[c*] Faculty of Natural Sciences and Engineering, University of Ljubljana, Slovenia
[d] Faculty of Chemistry and Chemical Technology, University of Ljubljana, Slovenia

(Received 21 November 2018; accepted 23 January 2019)

Abstract

In the present study, the corrosion mechanism of commercial FeCrAl alloy (Kanthal AF) during annealing in nitrogen gas (4.6) at 900 °C and 1200 °C is outlined. Isothermal and thermo-cyclic tests with varying total exposure times, heating rates, and annealing temperatures were performed. Oxidation test in air and nitrogen gas were carried out by thermogravimetric analysis. The microstructure is characterized by scanning electron microscopy (SEM-EDX), Auger electron spectroscopy (AES), and focused ion beam (FIB-EDX) analysis. The results show that the progression of corrosion takes place through the formation of localized subsurface nitridation regions, composed of AlN phase particles, which reduces the aluminum activity and causes embrittlement and spallation. The processes of Al-nitride formation and Al-oxide scale growth depend on annealing temperature and heating rate. It was found that nitridation of the FeCrAl alloy is a faster process than oxidation during annealing in a nitrogen gas with low oxygen partial pressure and represents the main cause of alloy degradation.

Keywords: *FeCrAl alloys; Alumina scale; Oxidation; Nitridation; Corrosion; AlN phase*

1. Introduction

FeCrAl – based alloys (Kanthal AF ®) are well known for their superior oxidation resistance at elevated temperatures. This excellent property is related to the formation of thermodynamically stable alumina scale on the surface, which protects the material against further oxidation [1]. Despite superior corrosion resistance properties, the lifetime of the components manufactured from FeCrAl - based alloys can be limited if the parts are frequently exposed to thermal cycling at elevated temperatures [2]. One of the reasons for this is that the scale forming element, aluminum, is consumed in the alloy matrix in the subsurface area due to the repeated thermo-shock cracking and reforming of the alumina scale. If the remaining aluminum content decreases beneath critical concentration, the alloy can no longer reform the protective scale, resulting in a catastrophic breakaway oxidation by the formation of rapidly growing iron-based and chromium-based oxides [3,4]. Depending on the surrounding atmosphere and permeability of surface oxides this can facilitate further internal oxidation or nitridation and formation of undesired phases in the subsurface region [5].

Han and Young have shown that in alumina scale forming Ni Cr Al alloys, a complex pattern of internal oxidation and nitridation develops [6,7] during thermal cycling at elevated temperatures in an air atmosphere, especially in alloys that contain strong nitride formers like Al and Ti [4]. Chromium oxide scales are known to be nitrogen permeable, and Cr_2N forms either as a sub-scale layer or as internal precipitate [8,9]. This effect can be expected to be more severe under thermal cycling conditions which lead to oxide scale cracking and reducing its effectiveness as a barrier to nitrogen [6].

The corrosion behaviour is thus governed by the competition between oxidation, which leads to the protective alumina formation/maintenance, and nitrogen ingress leading to internal nitridation of the alloy matrix by formation of AlN phase [6,10], which leads to the spallation of that region due to higher thermal expansion of AlN phase compared to the alloy matrix [9].

When exposing FeCrAl alloys to high

---

*Corresponding author: *blaz.karpe@omm.ntf.uni-lj.si*

DOI:10.2298/JMMB181121012V

temperatures in atmospheres with oxygen or other oxygen donors such as H_2O or CO_2, oxidation is the dominating reaction, and alumina scale forms, which is impermeable to oxygen or nitrogen at elevated temperatures and provide protection against their intrusion into the alloy matrix. But, if exposed to reduction atmosphere (N_2+H_2), and protective alumina scale crack, a local breakaway oxidation starts by the formation of non-protective Cr and Fe-rich oxides, which provide a favorable path for nitrogen diffusion into the ferritic matrix and formation of AlN phase [9].

The protective (4.6) nitrogen atmosphere is frequently applied in the industrial application of FeCrAl alloys. For instance, resistance heaters in heat treatment furnaces with a protective nitrogen atmosphere are an example of the widespread application of FeCrAl alloys in such an environment. The authors report that the oxidation rate of the FeCrAlY alloys is considerably slower when annealing in an atmosphere with low oxygen partial pressures [11].

The aim of the study was to determine whether annealing in (99.996%) nitrogen (4.6) gas (Messer® spec. impurity level O_2 + H_2O < 10 ppm) affects corrosion resistance of FeCrAl alloy (Kanthal AF) and to what extent it depends on the annealing temperature, its variation (thermal-cycling), and heating rate.

2. Experimental

The commercial FeCrAl ferritic alloy (Kanthal AF®) supplied by Sandvik Materials Technology AB, in the form of 0.7 mm thick cold-rolled sheet was used in the investigation. In addition to the main alloying elements (Al, Cr) it also contains small amounts of reactive metals like Ti, Y, and Zr for better alumina scale adherence and alloy creep resistance [12,13]. The chemical composition of the alloy is given in Table 1.

The specimens used in experiments were in the form of coupons, 10 x 20 x 0.7 mm in size, cut from sheet mechanically. All specimens were tested in the as-received condition. Before the tests, the specimens were only ultrasonically cleaned in acetone.

The specimens exposed to thermal cycling were tested in the thermomechanical simulator Gleeble 1500D. The temperature of the specimens was computer controlled and measured with S-type thermocouple in the center of the coupons surface. Before initialization of the experiments, the equipment was purged with 99.996% pure technical nitrogen gas flow for ten minutes.

Three series of experiments have been performed, as follows:

- Specimens were annealed at 1200 °C for one minute in ambient air or 99.996% pure nitrogen gas. Heating time to the required temperature was 5 seconds (heating rate 240 °C s^{-1}) and cooling time 30 seconds to reach 55 °C (cooling rate 40 °C s^{-1}, cooling with air or nitrogen gas stream).
- Isothermal annealing for one hour at a temperature of 1200 °C or 900 °C in (4.6) nitrogen gas. Heating and cooling procedure was the same as in the previously described experiment.
- Thermal cycling tests included heating the samples in the 4.6 nitrogen gas up to 1200 °C or 900 °C with the heating rate of 240 °C s^{-1}, holding at desired temperature for 18 seconds followed by cooling to 100 °C with cooling rate of 11 °C s^{-1}. To compare the results with isothermal annealing, the number of cycles (200 cy) was set to correspond to the time of one hour at the highest annealing temperature.

For comparison of the oxidation and nitridation kinetics in air or nitrogen atmosphere, mass gains were also measured by thermogravimetric method (Mettler Toledo TGA/DSC1) in a temperature interval from 25 °C to 1200 °C. The heating rate was 50 °C min^{-1}. Before annealing in a nitrogen atmosphere, the furnace chamber was purged with nitrogen gas (4.6) flow for 30 minutes. After dynamic measurements in nitrogen gas flow of 100 mL min^{-1}, samples were annealed at the final temperature for 1.5 or 10 minutes, respectively and cooled down under nitrogen gas flow with a cooling rate of 30 °C min^{-1}. The same heating and cooling procedure was also used when samples were annealed in an air atmosphere.

Metallographic characterization of the samples was carried out by scanning electron microscope (SEM). The elemental composition of the oxide layers and other phases in subsurface area was determined by energy dispersive X-ray spectroscopy (EDX) using an accelerating voltage of 10 keV and by Auger electron spectroscopy (AES, Auger electrons PHI SAM model 545A) using a 3 keV primary electron beam and an electron current of 1.0 μA. Analyses spot was 10 μm in diameter. Depth profiling over the region of 6 x 6 mm was also carried out by Ar ion sputtering with a beam of 1 keV. The sputtering rate was estimated to about 1 nm min^{-1} measured on Ni reference layer of known thickness. The oxide scale morphology was analysed by FIB-SEM DualBeam system, type FEI Helios Nanolab 650 equipped with the energy dispersive X-ray spectrometer (EDX).

Table 1. *The chemical composition of the commercial FeCrAl alloy (Kanthal AF)*

El.	Cr	Al	Si	Mn	S	Ni	Ti	Zr	Y	C	Ni	Fe
wt.%	22	5.3	0.17	0.18	0.004	0.27	0.06	0.068	0.023	0.03	0.27	Ball.

3.Results and discussion

3.1 Initial oxidation/nitridation in air or nitrogen atmosphere

All metals and alloys exposed to the air atmosphere have developed a few nanometers thick layer of oxide on the surface [14]. As can be seen from the AES depth profile of elements (Figure 1a), the surface is covered with 2-3 nm thick oxide scale. It is not possible to determine which oxide prevails on the surface, because there is no distinctive enrichment with one of the alloying elements and the oxide layer is very thin. During heating to an elevated temperature in air or (4.6) nitrogen atmosphere, this oxide scale quickly thickens. Figures 1b and 1c show AES depth profile of specimens heated to 1200 °C for 1 minute, with a heating rate of 240 °Cs^{-1}, in an air or nitrogen atmosphere. It can be seen, that after annealing in both atmospheres, the Al-oxide layer is formed on the surface. The thickness of the oxide scale after one-minute annealing at 1200 °C in air atmosphere is approximately 600 nm and in the (4.6)

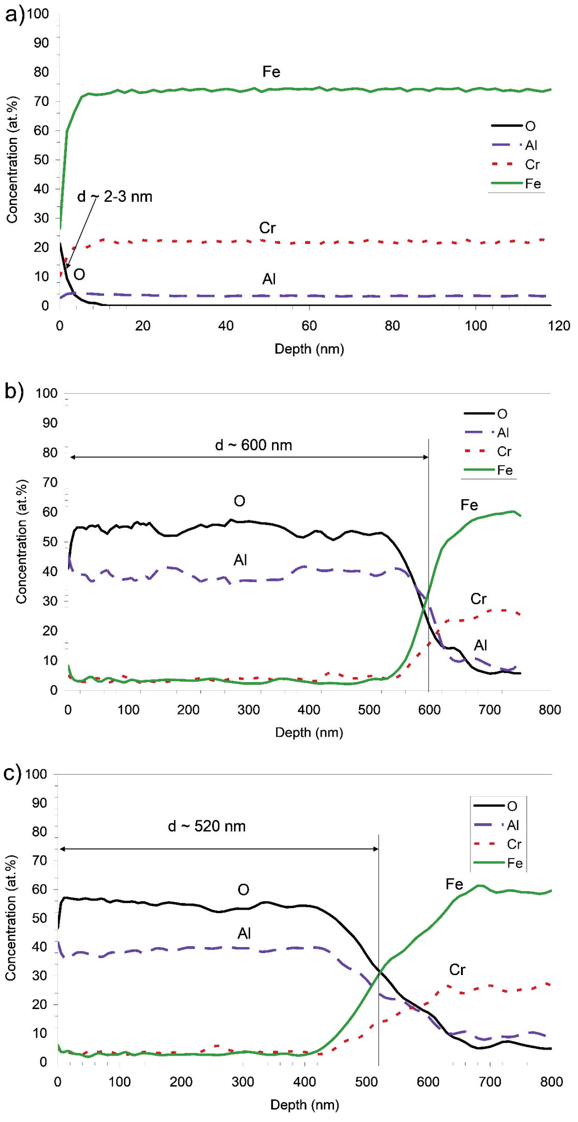

Figure 1. *AES depth profiles of elements showing the elemental composition of the oxides on Kanthal AF surface; (a) initial untreated surface, (b) 1 minute annealing in air at 1200 °C (240 °C s^{-1}), (c) 1 minute annealing in the N$_2$ gas at 1200 °C (240 °C s^{-1})*

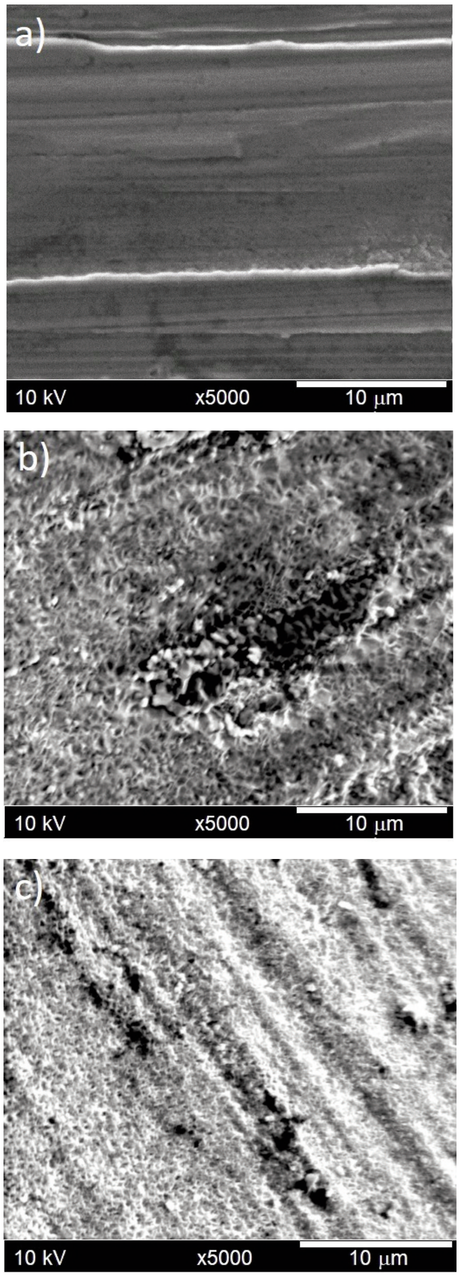

Figure 2. *Surface morphology of the specimens before and after annealing for 1 minute at 1200 °C; (a) initial untreated surface, (b) annealed in air atmosphere, (c) annealed in N$_2$ atmosphere (heating rate 240 °C s^{-1})*

nitrogen atmosphere around 520 nm. Despite very low partial pressure of oxygen in 99.996% (4.6) nitrogen atmosphere (<10 ppm), the activity of oxygen is steel sufficient to form thin alumina scale on the surface.

The surface morphology of the untreated specimen and specimens after 1 minute of annealing in an air or nitrogen atmosphere at 1200 °C is shown in Figure 2, and cross-sections in Figure 3. As can be seen, the surface is covered with a thin layer of Al_2O_3, confirmed by AES analysis. In some areas of the specimen surface, we found a layer of Fe rich oxide above the Al_2O_3 layer (Figures 3a, 3b), when annealed in an air atmosphere. Formation of the Fe rich oxides can be explained by missing or cracked alumina scale before annealing, and fast heating rate (240 °C s^{-1}), which cause that iron oxidation overtook the formation of protective alumina scale. During further annealing, aluminium oxide layer formed underneath Fe oxide by the aluminothermic reaction, but the time of exposure at elevated temperature was not sufficient to completely reduce the Fe-oxides. The Zr/Ti oxide particles incorporated in the alumina scale were also detected in some areas.

Figures 3c and 3d show subsurface microstructure of the sample annealed at 1200 °C in nitrogen gas. As we can see, a very small amount of oxygen is enough for the formation of the alumina scale, but the Al_2O_3 layer is thinner and separated. Of course, we do not exclude the possibility that it cracked during sample preparation. But on some localized subsurface regions of the sample, we also found AlN particles embedded in the alloy matrix, indicating that nitridation already started.

3.2 Thermogravimetric analysis

The thermogravimetric analysis was performed on specimens during annealing in nitrogen and air atmosphere, respectively. The mass gain curves are given in Figure 4. The mass gain per unit area for first 5 minutes of heating can be attributed to the buoyancy effects during the TGA measurement, due to the decrease in the density of the atmosphere in which the crucible floats [15]. The onset temperature for oxidation and nitridation/oxidation processes was similar for all samples and ranged between 880 °C to 920 °C. Final mass gains were determined from the

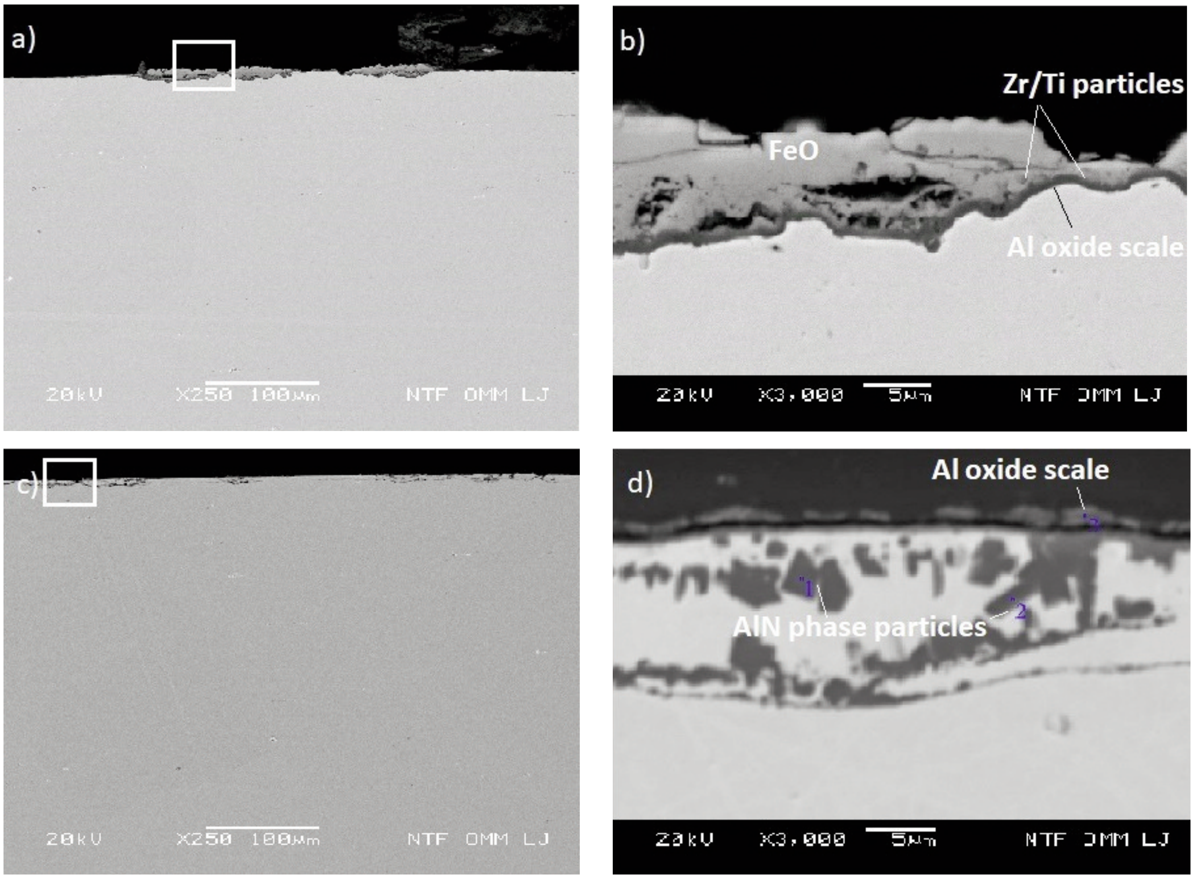

Figure 3. *Cross sections of FeCrAl alloy (Kanthal AF) samples after annealing for 1 minute at 1200 °C (240 °C s^{-1}): ,(a,b) annealing in air atmosphere, (b) higher magnification of marked detail on Figure 3a, (c,d) annealing in N_2 atmosphere, (d) higher magnification of marked detail on Figure 3c*

difference between the final mass after a certain time of the isothermal annealing and the mass of the sample at 900 °C. Calculated mass gains per unit area are given in Table 2. Because only traces of oxygen are sufficient for alumina scale formation, and measurements were carried out in the flow of nitrogen gas of limited purity, a certain amount of mass gain during annealing in nitrogen atmosphere can be contributed to oxidation. Namely, with longer annealing times, the difference in mass gains of the samples annealed in air or nitrogen decreases, indicating parabolic growth of oxide surface scale.

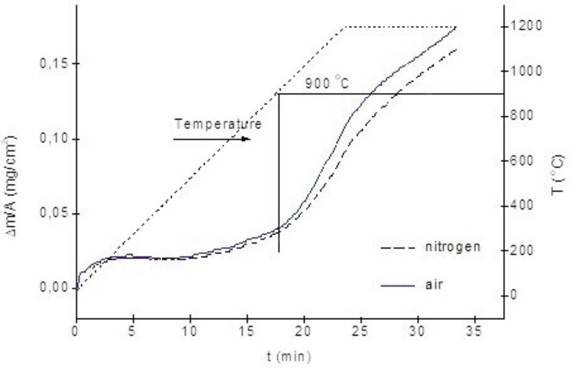

Figure 4. *Mass gain curves per unit area for FeCrAl alloy (Kanthal AF) as a function of time and atmosphere (annealed at 1200 °C in air or nitrogen atmosphere, heating rate 50 °Cmin^{-1})*

Table 2. *The mass gains (mg cm^{-2}) of FeCrAl alloy after heating in nitrogen or air flow at 1200 °C. The mass gains were determined from the difference between the final mass after a certain time of the isothermal annealing and the mass of the sample at 900 °C*

	nitrogen flow	air flow
After 1 min	0.066	0.080
After 5 min	0.097	0.108
After 10 min	0.124	0.135

3.3 Microstructure after isothermal annealing at 900 °C for 1 hour in N_2 atmosphere

Figures 5a, 5b, and 5c show the surface of FeCrAl alloy (Kanthal AF) sample after isothermal annealing at 900 °C for 1 h in N_2 atmosphere. Heating rate to annealing temperature was 240 °C s^{-1}. After one hour of isothermal annealing in N_2 gas, the sample surface was covered with the alumina scale. In addition, three distinctive morphological areas were also detected on the surface: areas covered by Cr/Mn-rich oxides (Figure 5b, area 1), regions covered by Fe-rich oxides (Figure 5b, area 2) and regions with Ti and Zr oxides embedded into alumina scale (Figure 5b, area 3), confirmed by EDXS analysis.

Figures 6a and 6b show a cross-section of the specimen after annealing for 1 hour at 900 °C in N_2 gas. Corroded regions, with the distinctive hemispherical pattern, spreading into the alloy matrix

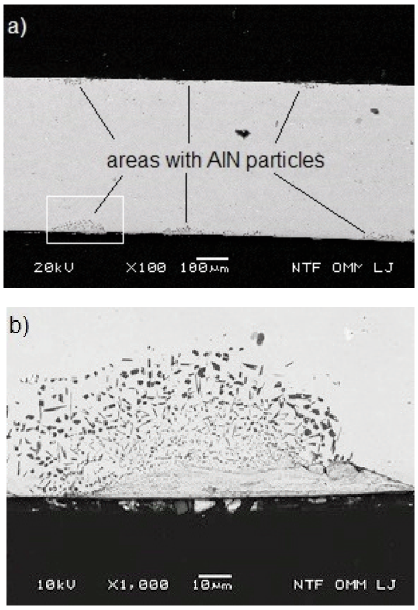

Figure 6. *(a) Cross section of Kanthal AF sample after annealing at 900 °C for 1 h in N_2 atmosphere, (b) marked detail*

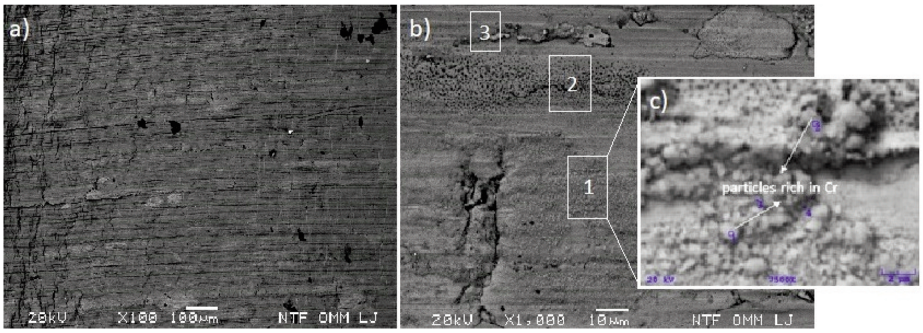

Figure 5. *Surface morphology of Kanthal AF sample isothermally annealed at 900 °C for 1 h in N_2 atmosphere, (a) surface morphology (low magnification), (b) areas with various phases, and (c) detail morphology of Cr-rich oxides*

for up to 70 µm are clearly visible. By SEM/EDXS spot analysis was revealed that these dark particles are the AlN phase.

The FIB cross-section shown in Figure 7a was prepared by eroding through the surface area covered with Cr/Mn-rich oxides. As we can see, needle-shaped particles, distributed in a hemispherical pattern were formed in the subsurface area. According to chemical composition (EDXS), the particles represent the AlN phase. This proves that chromium oxides are indeed permeable to nitrogen and represent one of the entering areas of nitrogen into the alloy matrix [9]. In addition, we also found alumina oxides on the matrix grain boundaries (internal oxidation), indicating that formation of the alumina layer on top of nitriding regions will be complicated and slower, due to aluminium depletion in those areas.

Figure 7b shows a thin layer, rimmed by AlN particles, below the alumina scale. We did not find any cracks in the alumina scale, which may act as nitrogen points-of-entry into the alloy. Since the layer is much thinner and has a different distribution of AlN particles than in the region below Cr/Mn-rich oxides, it led us to the conclusion that alumina scale is impermeable for nitrogen, but nitridation is a faster process than alumina scale formation during annealing at 900 °C in nitrogen atmosphere with low oxygen partial pressure. Furthermore, because AlN precipitates form a continuous rim at the certain distance from the surface (Figures 7b, 8a) and the central part of this layer has even lower content of Al than nominal composition of the alloy (Figure 8b), led us to the conclusion that AlN is also an obstacle for aluminium diffusion into this nitride rimmed layer. When aluminium in the matrix of this layer is consumed below the critical concentration, the AlN particles will start to disintegrate, because Al_2O_3 is thermodynamically more stable than AlN [8], and the counter concentration gradient of aluminum and nitrogen develops, forcing aluminium to diffuse towards the surface and nitrogen towards AlN rim, leaving the central part of the layer depleted.

Figure 8a shows the cross section of AlN rimmed layer below the alumina scale, formed after annealing a specimen for 1 hour at 900 °C in a N_2 atmosphere. Multi-layered structure is visible. A layer of oxide nodules on top, continuous alumina oxide scale in the middle, and a thin layer of aluminium depleted alloy matrix surrounded with AlN particles, distributed either as the continuous rim of particles at a certain distance from the surface or as separated particles below the oxide scale. Figure 8b shows the EDXS line concentration profile, marked on Figure 8a with a blue line. The AlN phase underneath oxide scale and in area "A" was confirmed by spot EDXS analysis (area A).

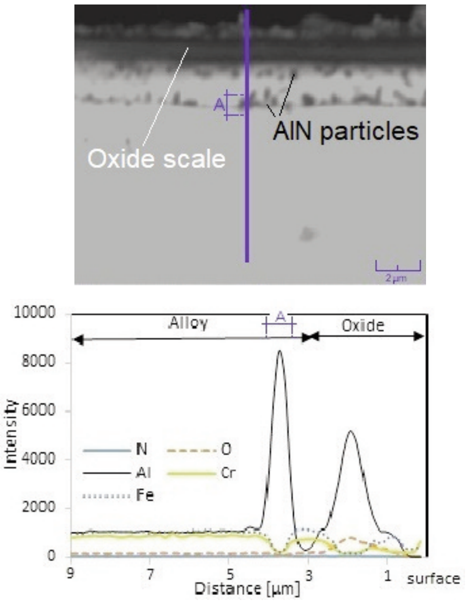

Figure 8. *(a) Detail of a subsurface area, (b) SEM/EDX line concentration profile, (annealed at 900 °C for 1 hour in N_2 atmosphere, heating rate 240 °C s^{-1})*

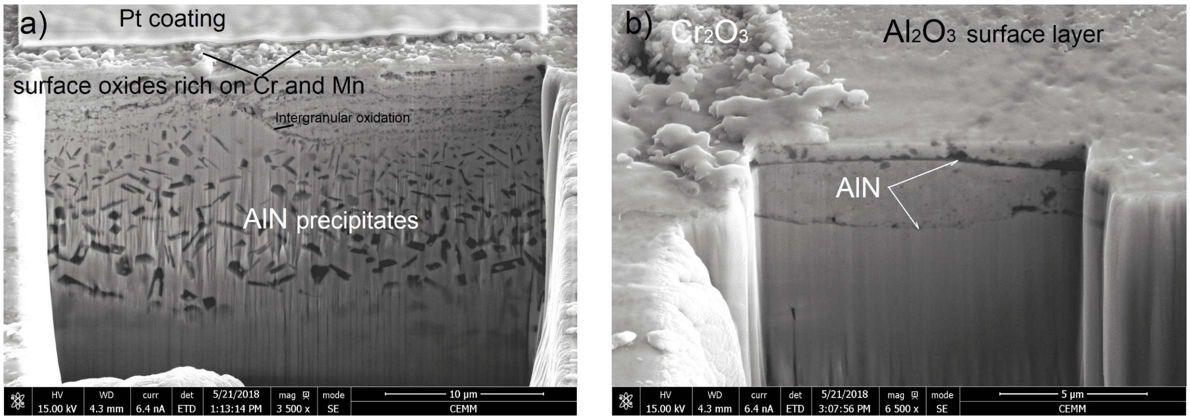

Figure 7. *3D FIB cross sections, (a) through a surface area covered with Cr/Mn-rich oxides, (b) AlN-rimmed layer below the Al_2O_3 surface scale (annealed at 900 °C for 1 hour in N_2 atmosphere, heating rate 240 °C s^{-1})*

3.4 Microstructure after isothermal annealing at 1200 °C for 1 hour in N_2 atmosphere

After 1 hour of isothermal annealing at 1200 °C in a nitrogen atmosphere with high heating rate of 240 °C s^{-1}, nitridation regions were scarce and shallow, without a distinctive hemispherical pattern, indicating that oxygen potential at 1200 °C is sufficiently high for fast oxidation and formation of protective alumina scale. On the other hand, when the samples were heated up to 1200 °C with 50 °C min^{-1} heating rate, nitridation regions with substantially larger AlN particles formed, even after much shorter annealing times than during annealing at 900 °C. Figures 9a, 9b, and 9c show cross-sections of the TGA samples after one, five and ten minutes of isothermal annealing at 1200 °C in N_2 gas. Corroded regions are clearly visible. This gives us a proof that the heating rate has a critical role in reaction kinetics of nitridation and oxidation. Nitridation is a faster process than alumina scale formation at lower temperatures and vice versa at a higher temperature. Once nitridated regions are formed during slower heating, the protective alumina scale on top of them will not form easily regardless of annealing temperature, because of reduced Al concentration in the alloy matrix in that region [4,8,10]. However, due to higher annealing temperature, further nitrogen ingress at this sites and diffusion into the matrix are faster, allowing growth of larger AlN particles. The nitridation regions, which preferentially formed below surface regions, covered by Cr-rich oxides, were confirmed by EDXS spot analysis, and also discovered by other authors [9].

3.5 Microstructure after thermal cycling up to 900 °C and 1200 °C in N_2 atmosphere

Figures 10a, and 10b show surface morphologies of Kanthal AF specimens after thermal cycling tests at 900 °C and 1200 °C. The number of above described cycles (200 cy) was set to correspond to the time of one hour at the annealing temperature. In both cases, the surface is covered with a thin and cracked layer of alumina scale, but with more revealed corrugated surface morphology, when higher temperature was applied. This indicates much faster growth of alumina scale at 1200 °C in the atmosphere with low oxygen partial pressure. Besides thicker alumina layer, areas with larger Cr/Mn oxides are also present on the surface, while in case of the thermally cycled sample up to 900 °C, Cr/Mn-rich oxides were smaller, even compared to isothermal annealing at 900 °C. Figure 11a clearly shows crack propagation along the outer rim of nitridated regions. Some of these regions have already spalled away. In samples, thermally cycled up to 1200 °C, fewer nitridation regions were observed, but with substantially larger AlN particles. Figure 11b shows crack propagation along AlN/matrix interface just before spallation.

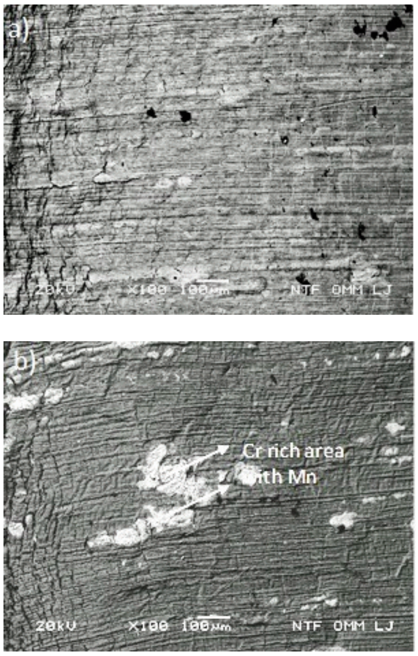

Figure 10. *Surface morphology of FeCrAl alloy (Kanthal AF) after thermal cycling in N_2 gas, (a) up to 900 °C, (b) up to 1200 °C (200 cycles, heating rate 240 °C s^{-1}, cooling rate 11 °C s^{-1})*

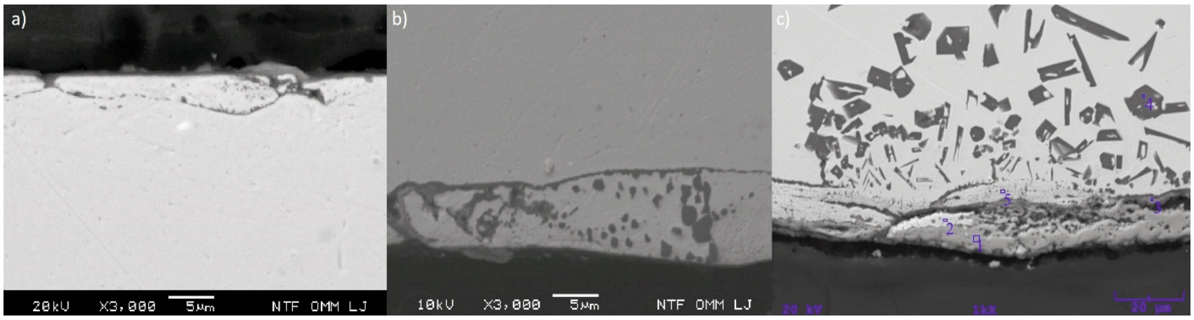

Figure 9. *Cross section of Kanthal AF sample after TGA measurements at 1200 °C in N_2 gas; (a) 1 min, (b) 5 min, (c) 10 min annealing (heating rate 50 °C min^{-1})*

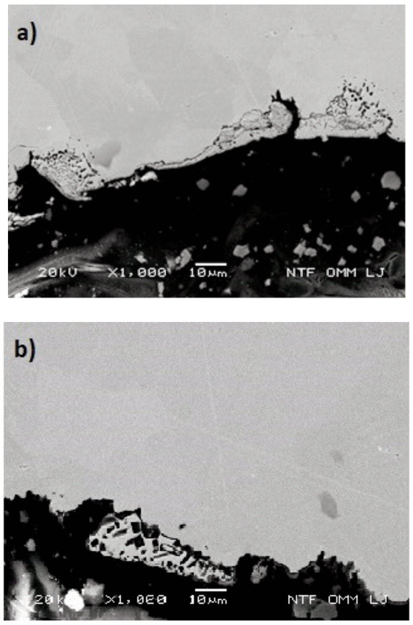

Figure 11. *Cross section of FeCrAl alloy (Kanthal AF) after thermal cycling in N_2 gas, (a) up to 900 °C, (b) up to 1200 °C; (200 cycles, heating rate 240 °C s^{-1}, cooling rate 11 °C s^{-1})*

4. Conclusions

In the present study, we focused on the early stages of corrosion of commercial FeCrAl alloy (Kanthal AF) during annealing at 900 °C and 1200 °C in (4.6) (99.996%) N_2 gas. The oxygen potential in (4.6) N_2 gas is still sufficiently high for the formation of alumina scale on the surface of the FeCrAl alloy, but the rate of its growth is slower than nitrogen ingress and formation of AlN phase at temperatures below 1200 °C. The proof for this is in the fact that the extent of corrosion products was greater after 1-hour isothermal annealing at 900 °C than at 1200 °C when high heating rate (240 °Cs^{-1}) was applied. The thermogravimetric measurements revealed that the onset temperature for oxidation and oxidation/nitridation processes was similar and ranged from 880 °C to 920 °C. Unfortunately, we could not differentiate between pure nitridation and oxidation during annealing in nitrogen gas of limited purity.

Corrosion appeared in the form of hemispherical nitridation regions, consisting of needle-shaped AlN particles embedded in the alloy matrix, which would spall away during thermal-cycling, due to the higher thermal expansion of AlN phase. Once nitridated regions were formed, the growth of the protective alumina scale on top of them was slow and complicated, regardless of annealing temperature, because of reduced Al concentration in the alloy matrix in that regions. Namely, when lower heating rate (50 °Cmin^{-1}) was applied to heat the sample up to 1200 °C, larger AlN particles formed, which is in accordance with much faster dissociation and diffusion of nitrogen at a higher temperature. The FIB and SEM/EDXS analysis revealed that Cr/Mn-rich oxides at the surface were the preferential points of nitrogen ingress into the alloy. Degradation occurred preferentially due to crack propagation along the AlN rim/matrix interface, which confirms the detrimental influence of AlN phase on the corrosion resistance of Kanthal AF alloy.

Acknowledgments

This work was supported by the Slovenian Research Agency through the project Selective plasma oxidation of alloys, ID L2-8181. Authors thank Tatjana Filipič for AES analyses and Maja Koblar for FIB analyses.

References

[1] W. J. Quadakkers, D. Naumenko, E. Wessel, V. Kochubey and L. Singheiser, Oxid. Met. 61, (2014), 17-37.

[2] I. Gurrappa, S. Weinbruch, D. Naumenko and W. J. Quadakkers, Mater. Corros. 51, (2000) 224-235.

[3] A. Dimyati, H. J. Penkalla, P. Untoro, D. Naumenko, W. J. Quadakkers, J. Mayer, Z. Metallkd. 94, (2003) 180-187.

[4] M. J. Bennett, J. R. Nicholls, N. J. Simms, D. Naumenko, W. J. Quadakkers, V. Kochubey, R. Fordham, R. Bachorczyk, D. Goossens, H. Hattendorf, A. B. Smith, and D. Britton, Mater. Corros. 56, (2005) 854-866.

[5] F. Liu, H. Götlind, J.E. Svensson, L.G. Johansson, M. Halvarsson, Oxid. Met. 67 (2007) 251-266.

[6] S. Han and D. J. Young, Mater. Res. 7, (2004) 11-16.

[7] N. Israelsson, K. A. Unocic, K. Hellström, T. Jonsson, M. Norell, J.E. Svensson and L. G. Johansson, Oxid. Met. 88, (2015),105-127.

[8] J. Enkvist, U. Bexell, M. Grehk and M. Olsson, Mater. Corros. 60, (2009) 876-881.

[9] C. Geers, V. Babic, N. Mortazavi, M. Halvarsson, B. Jönsson, L.G. Johansson, I. Panas, and J.E. Svensson, Oxid. Met. 87, (2017) 321-331.

[10] M. J. Bennett, R. Newton, and J. R. Nicholls,Mater. High Temp. 20, (2003) 347-356.

[11] D. J. Young, D. Naumenko, L. Niewolak, E. Wessel, L. Singheiser and W.J. Quadakkers, Mater. Corros. 61, (2010) 838-844.

[12] B. A. Pint, M. J. Dwyer, R. M. Deacon, Oxid. Met. 69, (2008) 211-231.

[13] X. Bao, L. Liu, S. Huang, Y. Jiang, X. Wang, L. Zhang, J. Min. Metall. Sect. B.53(1) B, (2017), 9-12.

[14] S. Petrović, B. Gakovič, J. Kovač, P. Panjan, E. Stratakis, M. Trtica, C. Fotakis, B. Jelenković, J. Mater. Sci. 49, (2014) 7900-7907.

[15] R. Cerc Korošec, P. Bukovec, Acta chim. 55, (2006) 136-147.

KOROZIJA PRI VISOKIM TEMPERATURAMA KOD KOMERCIJALNIH FeCrAl LEGURA (KANTHAL AF) U PRISUSTVU AZOTA

S. Veskovič – Bukudur[a], J. Kovač[b], B. Karpe[c*], P. Umek[b], A. Nagode[c], R. Cerc – Korošec[d], M. Bizjak[c]

[a] Hidria d.o.o., Idrija, Slovenija
[b] Institut Jozef Stefan, Ljubljana, Slovenija
[c*] Prirodno-tehnički fakultet, Univerzitet u Ljubljani, Slovenija
[d] Fakultet za hemiju i hemijsku tehnologiju, Univerzitet u Ljubljani, Slovenija

Apstrakt

U ovom radu je prikazan mehanizam korozije kod komercijalne legure FeCrAl (Kanthal AF) tokom postupka žarenja u prisustvu azota (4,6) na temperaturi od 900°C i 1200°C. Izvedeni su izotermalni i termo-ciklični testovi sa različitim ukupnim vremenom izlaganja, brzinama zagravanja, kao i temperaturama žarenja. Termogravimetrijskom analizom je ispitana oksidacija u kontrolisanoj atmosferi i uz prisustvo azota. Mikrostruktura je ispitana skenirajućim elektronskim mikroskopom (SEM), „Augerovom“ emisijskom spektroskopijom (AES), kao i fokusiranim jonskim zrakom (FIB-EDX). Rezultati pokazuju da se progresija korozije odvija tako što se stvaraju lokalizovani potpovršinski nitracioni delovi koji se sastoje od AlN faznih čestica koje smanjuju aktivnost aluminjuma, pri čemu on postaje krut i dolazi do lomljenja. Postupak stvaranja Al-nitrida i postepen rast Al-oksida zavise od temperature žarenja i brzine zagrevanja. Došlo se do zaključka da se postupak nitracije FeCrAl legure odvija brže od postupka oksidacije tokom žarenja u prisustvu azota pod niskim delimičnim pritiskom kiseonika, i da, samim tim, predstavlja glavni uzrok degradacije legure.

Ključne reči: *FeCrAl legure; Razmera aluminijuma; Oksidacija; Nitracija; Korozija; AlN faza.*